MAGNETIC IMAGING VIA SCANNING ELECTRON MICROSCOPY WITH POLARIZATION ANALYSIS†

R.J. Celotta, M. Scheinfein, J. Unguris and D.T. Pierce

Electron and Optical Physics Division
National Institute of Standards and Technology
Gaithersburg, Maryland 20899

INTRODUCTION

Scanning Electron Microscopy with Polarization Analysis (SEMPA) is a relatively new technique for obtaining images of magnetic microstructure. We will summarize the method and give a few examples of its application in this brief paper. A new review of the technique provides extensive additional information and references [1].

As in the magneto-optic Kerr technique, SEMPA images the magnetization of the sample directly, while Lorentz electron microscopy or magnetic force microscopy display magnetic structure through their sensitivity to magnetic fields. SEMPA was suggested as a technique [2,3] following the demonstration [3] that secondary electrons scattered from a ferromagnet by a high energy electron beam exhibited the spin polarization characteristic of the magnetization of the solid. It was envisioned that the highly focused electron beam of a scanning electron microscope could be rastered across a magnetic surface and a magnetization map would be obtained by measuring the polarization of the secondary electrons which are generated, as depicted in Fig 1. We use high efficiency polarization detectors based on the low energy diffuse scattering of electrons from a Au target [4] to measure all three components of magnetization. Other embodiments of SEMPA at KFA Jülich [5], Hitachi [6] and Stanford [7] use Mott or LEED polarization detectors.

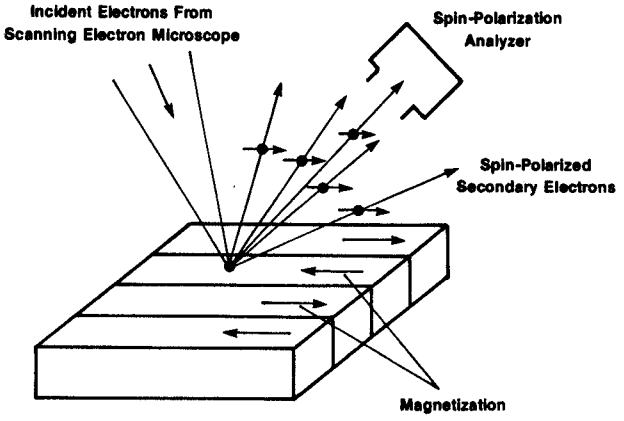

Fig. 1 A schematic representation of a SEMPA microscope.

SEMPA offers the ability to image the magnetic microstructure of solid samples with a resolution considerably better than optical techniques. A resolution of 40 nm has already been demonstrated for SEMPA [5] and 10 nm appears obtainable. This is to be contrasted with 1 μm resolution for the magneto-optical Kerr effect and about 10 nm for Lorentz microscopy when samples are thinned to less than 300 nm. Because SEMPA is based on measuring the polarization of secondary electrons which originate in the top few nm of the solid, it is intrinsically a surface analytic technique. As such, it requires that thick non-magnetic overlayers be removed and that measurements be made in an ultra-high vacuum environment. An advantage of the surface sensitivity is that very thin magnetic layers can be analyzed with no loss in signal. Because the magnetization images are obtained simultaneously with the topographic image, but are independent of the topographic measurement, the effect of surface physical structure on magnetic structure can be ascertained. Typically, a scanning Auger microscope is used so that an elemental map of the surface composition is also available. The time required for SEMPA imaging varies considerably depending on the magnetization and the resolution required. SEMPA images generally take a few minutes to acquire, although coarse (64x64) images can be obtained in one second for favorable cases. Both ferromagnetic and ferrimagnetic conductors can be imaged.

OBSERVATION OF THE (0001) SURFACE OF hcp COBALT

As an example of the three dimensional imaging capability of SEMPA, we show in Fig. 2 measurements [8] of the magnetic microstructure of a single crystal of Co that has been oriented so that its easy axis (c-axis) lies

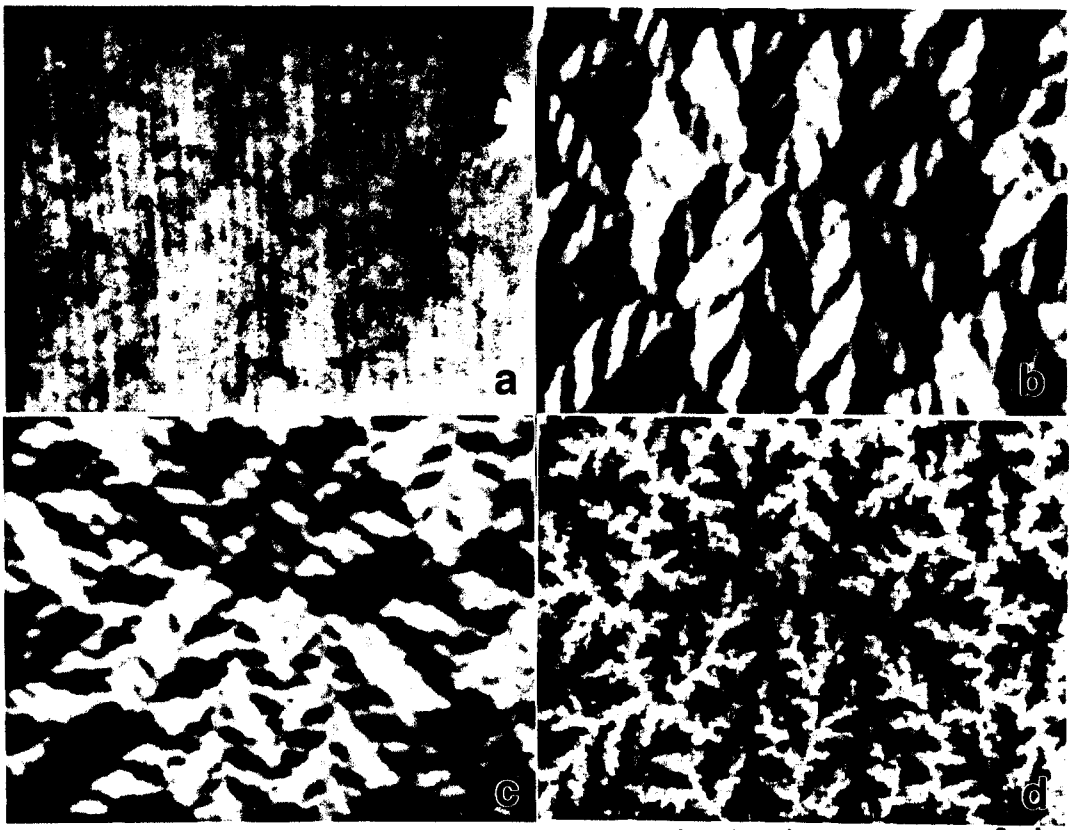

Fig. 2 Images of the topography (a) and the domain structure of the Co (0001) showing magnetization components (b) M_x along the horizontal and (c) M_y along the vertical in-plane directions, and (d) M_z in the out-of-plane direction. Each image is 18 μm wide.

perpendicular to the surface. Figure 2 (a) is the normal SEM topographic image obtained from the full secondary signal. Figures 2 (b), (c) and (d) show the M_x, M_y, and M_z components of the magnetization vector, respectively. The data are represented by a linear gray scale with white (black) indicating the maximum of the magnetization in the positive (negative) direction. Hence in the dendritic pattern of Fig. 2 (d), the white (black) areas represent magnetization out of (into) the crystal surface. The very different pattern shown by the in-plane magnetization components of Fig. 2 (b) and (c) can be analyzed by converting the value of these two components at each point to an in-plane angle and a magnitude. The angles appear quantized in roughly 60° increments which we speculate is related to a weak six-fold magnetocrystalline anisotropy. These patterns are very similar to those observed by the Kerr technique [9].

SURFACE DOMAIN WALLS IN Fe

The magnetostatic energy associated with magnetization perpendicular to the surface generally forces the magnetization at the surface to lie in the surface plane. Only for strong perpendicular anisotropies, as in Co above, do we see an out-of-plane component. For domain walls, this effect is seen in the rotation into the surface plane of the near-surface moments at the termination of a bulk Bloch wall. This results in a transition from a Bloch wall to a Néel wall within a length from the surface corresponding to approximately the width of a bulk Bloch wall. Figure 2 shows a SEMPA line scan across a 180° wall in Fe(100) between domains which are oriented in the $\pm y$ direction. The M_y component is directed along the domain direction. No perpendicular (M_z) component is observed. The M_x component shows the in-plane rotation of the magnetization for the surface Néel wall. The solid line is the result of our micromagnetics model calculation [10], broadened by the 70 nm beam probe width for this measurement. The calculation uses only the bulk values for the magnetization, the magnetocrystaline anisotropy and the exchange coupling constant. No magnetostriction or surface anisotropy terms were included. The excellent agreement obtained here, and in other systems with a wide range of magnetic parameters, gives us a high degree of confidence in our model calculations.

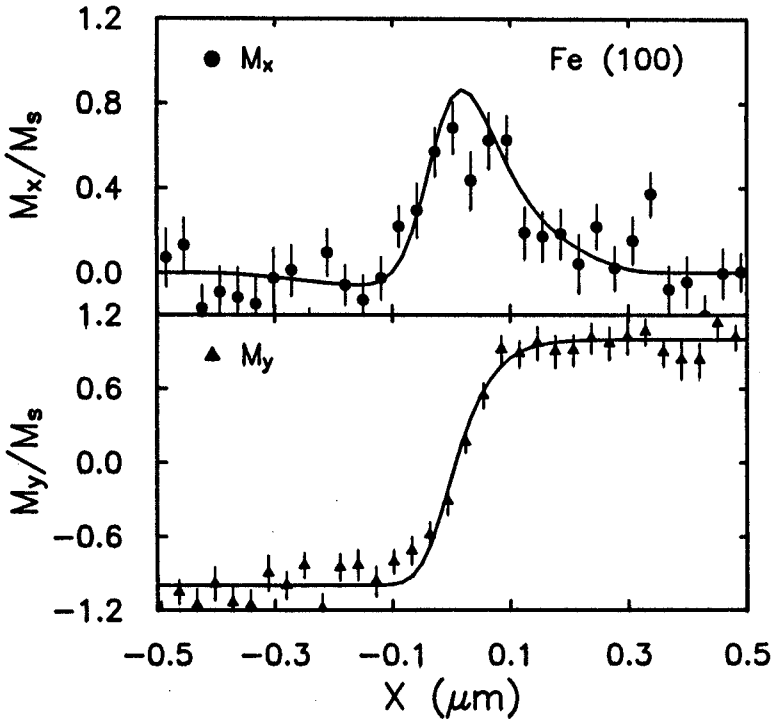

Fig. 3 Magnetization profile for 180° surface domain wall in Fe(100).

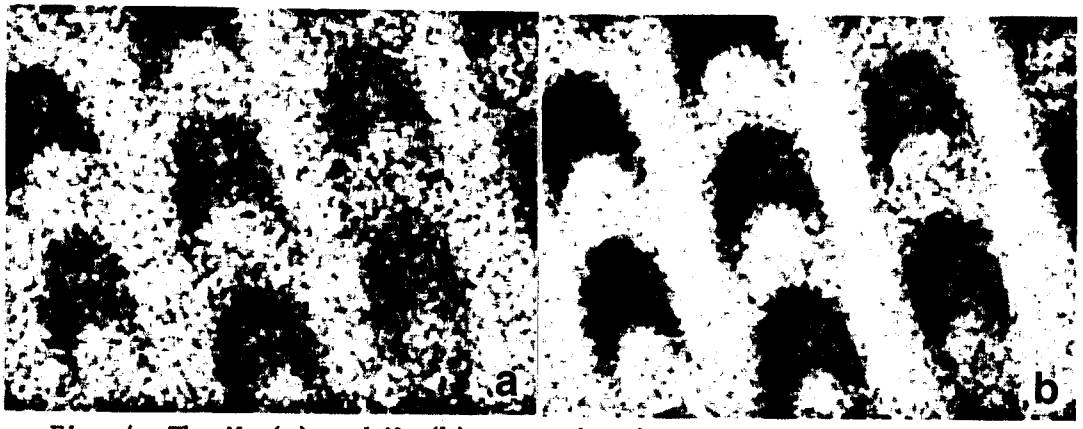

Fig. 4 The M_x (a) and M_z (b) magnetization components of laser written bits in a TbFeCo magneto-optic recording medium. Each image is 6.7 μm wide.

TbFeCo MAGNETO-OPTIC RECORDING MEDIA

The examples discussed so far have been ferromagnetic systems. The TbFeCo medium, as used for thermomagnetic writing in magneto-optical recording, is a ferrimagnetic system with its transition metal and rare earth sublattices antiferromagnetically aligned. A typical thermomagnetic material will have its compensation temperature, where the magnetization is zero, near room temperature. Figure 4 shows room temperature SEMPA images [11] of bits written in just such a material. The crescent shaped bits are created by reversing the applied magnetic field while the media is moved under a circular laser spot which provides local heating. We are able to see the domain structure even though there is no net magnetization because the secondary electrons analyzed in SEMPA come preferentially from the 3-d valence electrons in these alloys. The use of the Lorentz, MFM, and Bitter techniques near the compensation temperature is difficult because of the very small magnetic fields produced. SEMPA is being used here to study the size and shape of the written bits and the structure of their boundaries as a function of material and writing parameters.

REFERENCES

† This work was supported in part by the Office of Naval Research.

1. M.R. Scheinfein, J. Unguris, M.H. Kelley, R.J. Celotta and D.T. Pierce, Rev. Sci. Instrum. 61(10), October 1990.
2. R.J. Celotta and D.T. Pierce, in Microbeam Analysis 1982, ed. by K.F.J. Heinrich, (San Francisco Press, 1982) p. 469
3. J. Unguris, D.T. Pierce, A. Galejs and R.J. Celotta, Phys. Rev. Lettr. 49, 72 (1982).
4. M.R. Scheinfein, D.T. Pierce, J. Unguris, J.J. McClelland, R.J. Celotta and M.H. Kelley, Rev. Sci. Instrum. 60, 1 (1989).
5. H.P. Oepen and J. Kirschner, Phys. Rev. Lettr. 62, 819 (1989).
6. K. Koike, H Matsutama and K. Hayakawa, Scanning Micro. Intern., Supp. 1, 241 (1987).
7. T. VanZandt, R. Browning, C.R. Helms, H. Poppa, M. Landolt, Rev. Sci. Instrum. 60, 3430 (1989).
8. J. Unguris, M.R. Scheinfein, R.J. Celotta and D.T. Pierce, Appl. Phys. Lett. 55, 2553 (1989).
9. A. Hubert, R. Schäfer and W. Rave, Chin. J. Phys. Suppl. (to be published).
10. M. R. Scheinfein, J. Unguris, D.T. Pierce and R. J. Celotta, J. Appl. Phys. 67, 5932 (1990).
11. M. Aeschlimann, M.R. Scheinfein, J. Unguris, F.J.A.M. Greidanus, S. Klahn (to be published).